Available online at www.sciencedirect.com
ScienceDirect
Biochemical and Biophysical Research Communications 349 (2006) 1125–1129
BBRC
www.elsevier.com/locate/ybbrc

Crystal structure of human dynein light chain Dnlc2A: Structural insights into the interaction with IC74

Jun-Feng Liu, Zhan-Xin Wang, Xin-Quan Wang, Qun Tang, Xiao-Min An, Lu-Lu Gui, Dong-Cai Liang *

National Laboratory of Biomacromolecules, Institute of Biophysics, Academia Sinica, Beijing 100101, People's Republic of China

Received 18 August 2006
Available online 5 September 2006

Abstract

The human light chain of the motor protein dynein, Dnlc2A, is also a novel TGF-β-signaling component, which is altered with high frequency in epithelial ovarian cancer. It is an important mediator of dynein and the development of cancer, owing to its ability to bind to the dynein intermediate light chain (DIC) IC74 and to regulate TGF-β-dependent transcriptional events. Here we report the 2.1-Å crystal structure of Dnlc2A using single anomalous diffraction. The proteins form a homodimer in solution and interact mainly through the helix α_2, strand β_3, and the loop following this strand in each protein to generate a 10-stranded β-sheet core. The surface of the β-sheet core is mainly positively charged and predicted (by software PPI-Pred) to be the site that interacts with other partners. At the same time, the residues 79–82, 88, and 90 of each molecule formed two holes in the core. Residue 89 of each molecule, which is crucial for the DIC binding function of Dnlc2A, is within the holes. On the basis of these observations, we propose that the homodimer is the structural and functional unit maintained by hydrogen bonding interactions and hydrophobic packing, and that the patch of the surface of the β-sheet core is the main area of interaction with other partners. Furthermore, the two holes would be the key sites to interact with IC74.

Keywords: Dnlc2A; SAD; PPI-Pred

Cytoplasmic dyneins are microtubule-based motor proteins, moving to the minus end of microtubules, and are involved in various types of intracellular transport. They are large protein complexes consisting of heavy chains, and various intermediate and light chain subunits [1]. Three distinct classes of light chains (LCs), LC8, Tctex1/Tctex2, and Roadblock/LC7, have been shown to bind to distinct regions of IC74 [2].

As with other motor protein subunits, the roadblock light chain is crucial for the proper functioning of the Cytoplasmic dynein complex [3]. Roadblock/LC7 sequences from most species share more than 50% identity. These proteins belong to an ancient protein superfamily that is widely represented in archaea and bacteria, and may be involved in regulation of NTPase activity [4].

A human homologue of robl/LC7, Dnlc2A, has been identified, and its changes in expression in hepatocellular carcinoma have been recorded [5]. Dnlc2A is also a novel TGF-β-signaling component (termed km23), a protein that interacts with TGF-β receptor II [6]. Km23 mutations were detected in eight of 19 patients with ovarian cancer, representing an overall mutation rate of 42.1%. Such a high mutation rate suggests that km23 may play an important role in either TGF-β resistance or tumor progression in this disease [7]. The structure of Dnlc2A will give information on the ways that it interacts with its partners such as IC74 and TGF-β receptor II.

Three Dnlc2A NMR structures (two from human and one from mouse) that were solved recently all belong to the structure superfamily of Roadblock/LC7 [8,9]. The specific functions of these proteins vary substantially, but they have at least one feature in common, namely their involvement in multiple protein–protein interactions. Therefore,

* Corresponding author. Fax: +8610 64889867.
E-mail address: dcliang@sun5.ibp.ac.cn (D.-C. Liang).

0006-291X/$ - see front matter © 2006 Elsevier Inc. All rights reserved.
doi:10.1016/j.bbrc.2006.08.161

this fold seems to be common to proteins that have a variety of dissimilar functions but are all involved in protein–protein interactions. The crystal structure of Dnlc2A will give information on the ways it and other members of the superfamily interact with its partners.

We now report the three-dimensional structure of the homodimeric Dnlc2A at 2.1-Å resolution using single anomalous diffraction. This report is the first to present the crystal structure of Dnlc2A and lays the foundation for understanding how this small scaffold protein mediates several interactions with proteins that are important components of dynein function and cancer development.

Materials and methods

Cloning, expression, and purification. The expression vector pET-Dnlc2A was constructed by the Shanghai Institute of Hematology. The protein was produced in an *Escherichia coli* strain, BL21 (DE3), that was transformed with the expression vector. Cells were grown on LB media containing 100-μg/μl ampicillin at 37 °C to an A600 of 0.6 and then induced with 1 mM isopropyl β-D-thiogalactoside for 3 h. Cells were harvested by centrifugation, resuspended in buffer (500 mM NaCl, 50 mM Tris–HCl, pH 8.0), and disrupted by sonication. The extract was centrifuged for 15 min at 10,000*g*. The protein was purified by column chromatography in two steps using a Ni-affinity column and a Superdex 75 gel-filtration column (Amersham Pharmacia Biotech).

SDS–PAGE showed one band around 12 kDa corresponding to the molecular mass of Dnlc2A, and gel-filtration column analysis confirmed this by showing a monodisperse peak of the dimer size.

Crystallization and data collection. Crystallization experiments were performed using the hanging-drop vapor diffusion method. Crystallization conditions were screened using the sparse-matrix sampling [10]. Crystals were obtained in a system using PEG4000 as a precipitant. After optimization of the crystallization conditions, crystals were obtained by mixing 2 μl protein solution (10 mg/ml, 0.5 mM DTT, 500 mM NaCl, and 50 mM Tris, pH 8.0) with 2-μl reservoir solution at 291 K. The reservoir solution was 28% PEG 4000, 0.1 M CeCl, and 0.1 M Tris, pH 7.6.

The X-ray diffraction data were collected from a single flash-frozen (100 K) crystal at a resolution of 2.1 Å. The data were processed with DENZO and SCALEPACK software [11]. The crystal belonged to the space group $P6_1$, with unit-cell parameters of $a = b = 83.1$ Å, and $c = 98.1$ Å. There were two molecules in the crystallographic asymmetric unit. The statistics are listed in Table 1.

Structure determination and refinement. The program *Phenix* [12] was used to locate the cesium sites in the crystal and to calculate initial phases. Using the improved phases and the structure factors from the SAD data set, automated model building was initialed with ARP/Warp [13] and the calculated map was good enough to trace most of the protein's main chains and side chains. Further model adjustment was performed by using the program Coot [14]. The structural refinement was carried out with the program refmac [15,16]. After several cycles of refinement and model rebuilding, as well as B factor refinement, a final model consisting of 177 residues and 146 water molecules with an *R*-factor of 0.203 and an *R* free of 0.235 was obtained. Assessment of the final model using the program PROCHECK [17] showed that 89.6% of the residues were in the most favorable region and no residues were in the disallowed region. The refinement statistics are shown in Table 1.

Table 1
Data collection and refinement statistics

Data collection	
Wavelength (Å)	1.5418
Resolution (Å)	10.0–2.10
Redundancy	275601 (12.5)
Unique reflections	21991
Completeness (%)	99.5 (98.6)
$I/\sigma(I)$	28.6 (7.1)
R_{merge} (%)	0.083 (0.428)
Phasing and refinement	
Maximum resolution (Å) for phasing	2.1
Space group	$P6_1$
No. of Ce atom in asu	1
FOM after density modification	0.845
Refinement statistics	
Resolution (Å)	10.0–2.1 Å
Unique reflections	21991
R factor	0.203
R_{free}	0.230
No. of atoms	
Protein	1376
Water	146
Ce	1
r.m.s. deviation	
Bond distance (Å)	0.013
Angle distance (°)	1.368
Overall average B factor (Å^2)	29.9
Residues in most favored region	156 (89.5%)
Residues in additional allowed regions	21 (10.5%)

Results and discussion

Description of the structure

The crystal structure of Dnlc2A reveals a homodimer with a non-crystallographic twofold axis of symmetry (Fig. 1). Each of the monomers of Dnlc2A folds as a compact domain and consists of a central five-stranded antiparallel β-sheet, β_1 (18–23), β_2 (30–32), β_3 (67–73), β_4 (77–81), and β_5 (86–92) sandwiched between α-helix α_2 (36–60) on one side and the terminal helices α_1 (6–13) on the other side. The strand order is 2 1 5 4 3. The electron density for the N terminal (the His tag, residues A1–8 and B1–5), residues A83–85, B84–85, and the C terminal (residues A96 and B96) is not well defined and should be considered as very flexible.

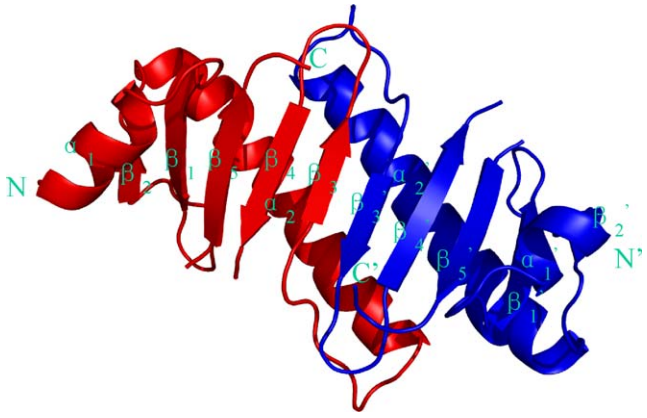

Fig. 1. The dimer structure of Dnlc2A. Illustration prepared with Pymol [20].

Characterization of the dimer interface

The two molecules in the asymmetric unit are related by a non-crystallographic twofold axis and are superimposable with a root mean square deviation of 0.41 Å over all C atoms of residues 8–95.

The dimer of Dnlc2A associates to form a continuous, antiparallel 10-stranded sheet with strand order 2 1 5 4 3 3* 4* 5* 1* 2* (the asterisk denotes molecule B). One side of the central β-sheet is covered by α2-helix bundles, α_2 and α_2', whereas the other side is covered by the α_1/α_1' two-helix bundle (Fig. 1).

The residues that form the interface are primarily within a contiguous stretch encompassing helix α_2, strand β_3, and the loop following this strand. The homodimer is maintained by hydrogen bonding interactions and hydrophobic packing. The intermolecular hydrogen bonds are, to a large extent, between the backbone atoms and side chains of the two-strand β_3, and the loop following this strand. Twenty intermolecular hydrogen bonds between them are formed, in the two monomers, respectively. Residues 61, 64, 65, 67, 68, 70, 72, and 74–76 in strand β_3 and the loop are involved in the interface formation (Fig. 2). A network of hydrogen bonds pointing towards this interface strongly stabilizes the interaction between monomers.

There are two layers in the dimer structure ($52 \times 25 \times 22$ Å). One layer is formed by the two α_2/α_2', and the other by the continuous, antiparallel 10-stranded sheet.

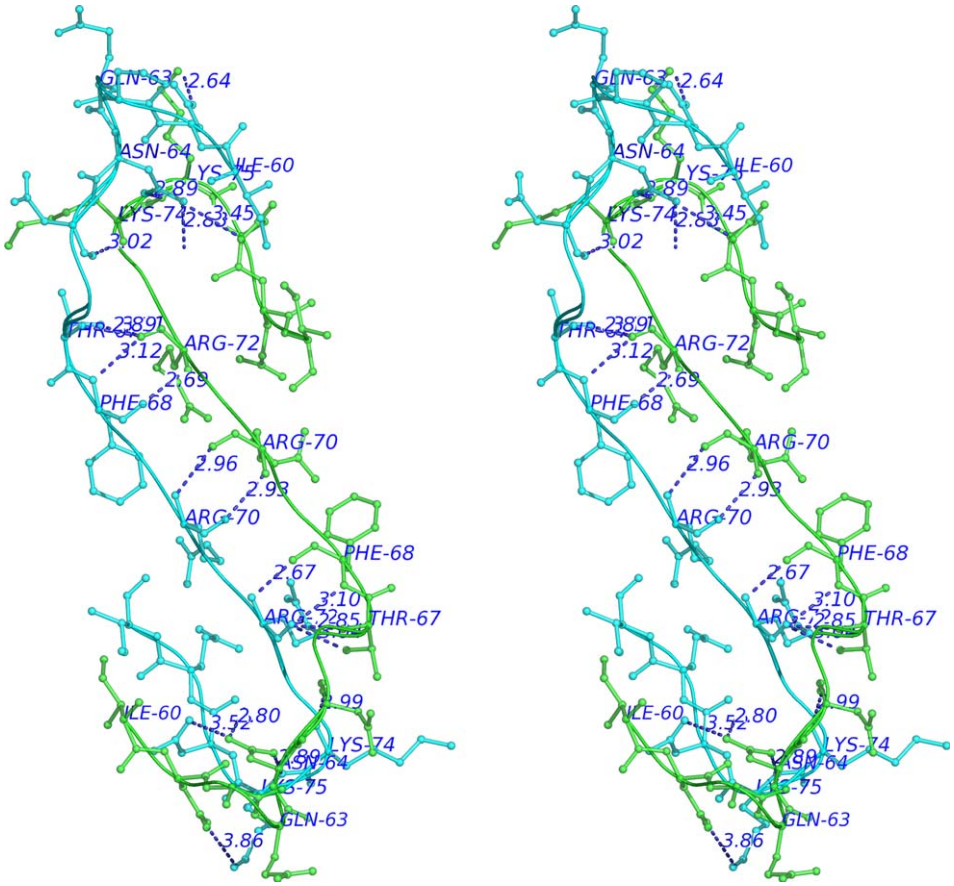

Fig. 2. Apparent networks of hydrogen bonds at the interface of monomer–monomer interactions of Dnlc2A (residues from 60 to 78). Apparent hydrogen bonds are denoted with dots (···) and the distance (d_H) in Å is indicated. The illustration was prepared with Pymol [20].

Table 2
The potential interaction pockets of Dnlc2A

Chain	Patch	Number	Residues
A	I	18	67T,68F,70R,82P,81A,79M,88L,80V,92Q,22V,8L,11L,90V,14Q,31K,7T,15K,17V
	II	16	52K,53A,70R,69L,49F,71I,48S,72R,73S,78I,46M,45L,44S,76N,42Y,41Q
	III	13	60I,59D,61D,62A,64N,56T,65D,67T,66L,57V,52K,53A,69L
B	I	17	8L,11L,88L,90V,86Y,14Q,17V,92Q,79M,80V,81A,83D,68F,67T,82P,70R,69L72R
	II	18	34M,18Q,70R,42Y,91I,,41Q,76N,75K,69L,48S,45L,78I,73S,74K,71I,49F,46M
	III	14	68F,67T,66L,65D,69L,64N,62P,59D,52K,53A,57V,61D,56T,60I

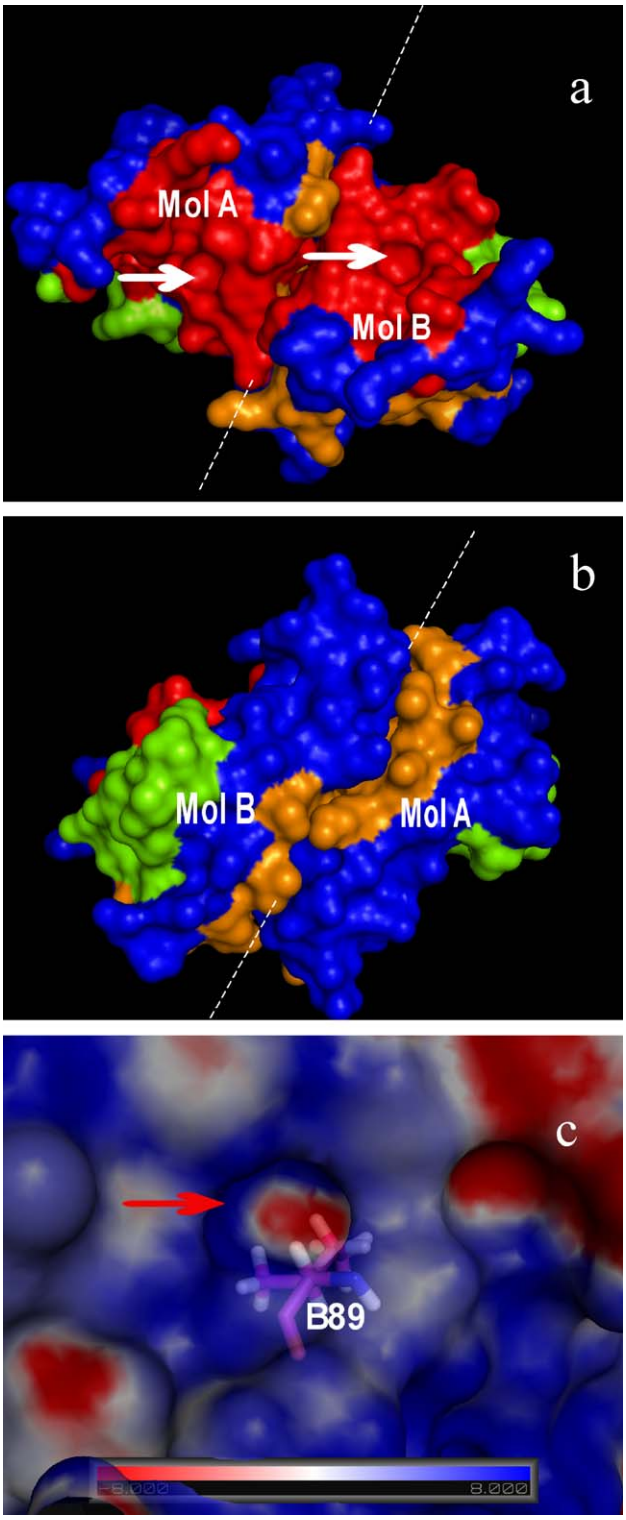

Fig. 3. The map of the potential interaction pockets of Dnlc2A and the dimer interface formed by them. (IA and IB:red; IIA and IIB: brown). (a) The residues to form the holes of the potential interaction pockets (IA and IB) and the dimer interface formed by IIA and IIB (on the site of sheet); (b) the dimer interface formed by IIA and IIB (on the site of helix); (c) the electrostatic surface potential of hole in the patch of IB. The molecular surface was created by the program APBS (red, negative; blue, positive; white, uncharged). (For interpretation of the references to color in this figure legend, the reader is referred to the web version of this paper.)

Structural alignment

A DALI [18] search found similarities to numerous proteins with a Profilin-like fold (SCOP 55769). A structural superposition of these structures clearly shows that all three structures represent the same fold.

The top DALI hits are from the Roadblock/LC7 domain (Protein Data Bank code 1SKO-B, *Z*-score 11.3, r.m.s.d. for 89 C_α atoms = 2.5 Å, sequence identity 12%) and (Protein Data Bank code 1J3W-A, *Z*-score 10.2, r.m.s.d. for 90 C_α atoms = 2.2 Å, sequence identity 10%) and (Protein Data Bank code 1SKO-A, *Z*-score 9.4, r.m.s.d. for 86 C_α atoms = 2.4 Å, sequence identity 9%). Besides overall deviation between the structure of Dnlc2A and other known structures of the proteins with a Profilin-like fold, there is a significant difference at the C terminus. In this region, structures other than Dnlc2A have an additional C-terminal α-helix.

There are also considerable structural similarities to other proteins. They are Profilin (actin-binding protein) (Protein Data Bank code 3NUL, *Z*-score 7.6, r.m.s.d. for 81 C_α atoms = 2.5 Å, sequence identity 6%) and (Protein Data Bank code 1PNE, *Z*-score 6.5, r.m.s.d. for 83 C_α atoms = 3.4 Å, sequence identity 10%).

These structures belong to the two superfamily of Roadblock/LC7 domain [103196] and Profilin [55770].The difference between them is that Profilin has two additional β sheets in the middle of the structure, which block the formation of the normal monomer–monomer interaction surface.

The crystal structure of Dnlc2A was compared with the ten conformers of the NMR-derived solution structure of human Dnlc2A deposited in the PDB with the Accession code 1Z09 [8].

The secondary-structure elements assigned to the structures of Dnlc2A in the crystalline state and in solution are not in good agreement. The r.m.s.d values of the main chain of 8 out of 14 are greater than 3.0 Å. This may be why the solution could not be obtained by molecular replacement using homology models from NMR.

At the same time, there are a number of hydrogen bonds that are present only in the X-ray structure. For example, residues 64, 67, 74, and 75 interact, respectively, with residues 73, 72, 65, and 64 in the crystal, whereas these interactions do not occur in the solution structure.

Implications for protein–protein interactions

The specific functions of these proteins of the Roadblock/LC7 domain vary substantially, but they have at least one feature in common, namely their involvement in multiple protein–protein interactions. Therefore, this fold seems to be common to proteins that have a variety of dissimilar functions but are all involved in protein–protein interactions. The PPI-Pred was used to predict the potential protein-binding pocket [19]. Table 2 lists the residues that make up the three highest-scoring patches of molecules A and B (patch

IA, IIA, IIIA, IB, IIB, and IIIB) (Fig. 3a and b). Fourty-nine residues involved the interaction between Dnlc2A and its partner (Table 2 and Fig. 3a). The highest-scoring patches (IA and IB) are linked together to form a large patch that covers nearly the entire continuous, antiparallel 10-stranded sheet. There is a small wide hole in the center of each binding patch, which is formed by residues 68, 69, 79–81, and 88–90 from three-β sheet (β_3, β_4, and β_5). The holes are only about 5 Å in depth and their radius is about 3 Å, into which a residue can fit (Fig. 3a and c). This surface has a positive electric charge, which may interact with other proteins by means of a salt bridge.

Through an NMR titration experiment, the residues on the β_3 and β_4 strands of Dnlc2A all have the largest chemical shift perturbations when IC74 is added [8]. All these residues are in the patches (IA and IB) involving the protein–protein interaction predicted on the basis of the crystal structure (Table 2 and Fig. 3a). In addition, I89 is crucial for the DIC binding function of km23 [9]. I89 is in a positively charged hole formed by the residues besides I89 such as 79–82, 88, and 90 (Fig. 3c). These residues are all predicted to interact with other proteins based on the crystal structure solved here.

In summary, the 10-stranded sheet formed by the two patches (IA and IB) is the main area that may be a likely site for additional protein–protein interactions. Two small holes, surrounded by residues 79–82, 88, 90, and with residue 89 within, are the key areas for the binding of IC74. That homodimer is the structural and functional unit maintained by hydrogen bonding interactions and hydrophobic packing.

Acknowledgments

This work was supported by the National Natural Science Foundation of China (NSFC) Nos. 30130080, 30200046; 973 project No. 2002CB713801; Chinese High Tech Research and Development (863) Program No. 2001AA233021, and KSCX1-SW-17 from the Ministry of Science and Technology of China (MOST) as well as fund from the Chinese Academy of Science (CAS). We wish to thank Mr. Han Yi, for his help during diffraction data collection. We also wish to thank Dr. Qiuhua Huang of the Shanghai Institute of Hematology for the expression vector construction. We are grateful to Miss Li Yuan of our laboratory for recombinant protein expression and expression. The atomic coordinate and structure factor of the structure of Dnlc2A has been deposited in the Protein Data Bank as 2HZ5.

References

[1] A.B. Bowman, R.S. Patel-King, S.E. Benashski, J.M. McCaffery, L.S. Goldstein, S.M. King, Drosophila roadblock and Chlamydomonas LC7: a conserved family of dynein-associated proteins involved in axonal transport, flagellar motility, and mitosis, J. Cell Biol. 146 (1999) 165–180.

[2] L.M. DiBella, M. Sakato, R.S. Patel-King, G.J. Pazour, S.M. King, The LC7 light chains of chlamydomonas flagellar dyneins interact with components required for both motor assembly and regulation, Mol. Biol. Cell 15 (2004) 4633–4646.

[3] S.J. Susalka, K. Nikulina, M.W. Salata, P.S. Vaughan, S.M. King, K.T. Vaughan, K.K. Pfister, The roadblock light chain binds a novel region of the cytoplasmic Dynein intermediate chain, J. Biol. Chem. 277 (36) (2002) 32939–32946.

[4] E.V. Koonin, L. Aravind, Dynein light chains of the Roadblock/LC7 group belong to an ancient protein superfamily implicated in NTPase regulation, Curr. Biol. 10 (2000) R774–R776.

[5] J. Jiang, L. Yu, X. Huang, X. Chen, D. Li, Y. Zhang, L. Tang, S. Zhao, Identification of two novel human dynein light chain genes, DNLC2A and DNLC2B, and their expression changes in hepatocellular carcinoma tissues from 68 Chinese patients, Gene 281 (2001) 103–113.

[6] W. Ding, K.M. Mulder, Km23: a novel TGFβ signaling target altered in ovarian cancer, Cancer Treat. Res. 119 (2004) 315–327.

[7] Q. Jin, W. Ding, C.M. Staub, G. Gao, Q. Tang, K.M. Mulder, Requirement of km23 for TGFβ-mediated growth inhibition and induction of fibronectin expression, Cell Signal. 17 (2005) 1363–1372.

[8] U. Ilangovan, W. Ding, Y. Zhang, C.L. Wilson, J.C. Groppe, J.T. Trbovich, J. Zuniga, B. Demeler, Q. Tang, G. Gao, K.M. Mulder, A.P. Hinck, Structure and dynamics of the homodimeric dynein light chain km23, J. Mol. Biol. 352 (2005) 338–354.

[9] J. Song, R.C. Tyler, M.S. Lee, E.M. Tyler, J.L. Markley, Solution structure of isoform 1 of Roadblock/LC7, a light chain in the dynein complex, J. Mol. Biol. 354 (5) (2005) 1043–1051.

[10] J. Jancarik, S.H. Kim, Sparse matrix sampling: a screening method for crystallization of proteins, J. Appl. Crystallogr. 24 (1991) 409–411.

[11] Z. Otwinowski, W. Minor, Processing of X-ray diffraction data collected in oscillation Mode, Methods Enzymol. 276 (1997) 307–326.

[12] P.D.R.W. Adams, L.-W. Grosse-Kunstleve, T.R. Hung, A.J. Ioerger, N.W. McCoy, R.J. Moriarty, J.C. Read, N.K. Sacchettini, T.C. Sauter, Terwilliger, PHENIX: building new software for automated crystallographic structure determination, Acta Cryst. D58 (2002) 1948–1954.

[13] R.J. Morris, A. Perrakis, V.S. Lamzin, ARP/wARP and automatic interpretation of protein electron density maps, in: C.W. Carter, R.M. Sweet (Eds.), Methods Enzymol. 374 (2003) 229–244.

[14] P. Emsley, K. Cowtan, Coot: model-building tools for molecular graphics, Acta Cryst. D 60 (2004) 2126–2132.

[15] G.N. Murshudov, A.A. Vagin, E.J. Dodson, Refinement of macromolecular structures by the maximum-likelihood method, Acta Cryst. D53 (1997) 240–255.

[16] Collaborative Computational Project, Number 4. "The CCP4 Suite: Programs for Protein Crystallography. Acta Cryst. D 50 (1994) 760–763.

[17] R.A. Laskowski, M.W. MacArthur, D.S. Moss, J.M. Thornton, PROCHECK: a program to check the stereochemical quality of protein structures, J. Appl. Crystallogr. 26 (1993) 283–291.

[18] L. Holm, C. Sander, Touring protein fold space with Dali/FSSP, Nuclic Acids Res. 26 (1998) 316–319.

[19] J.R. Bradford, D.R. Westhead, Improved prediction of protein–protein binding sites using a support vector machines approach, Bioinformatics 21 (2005) 1487–1494.

[20] W.L. DeLano, The PyMOL Molecular Graphics System (2002) DeLano Scientific, San Carlos, CA, USA. http://www.pymol.org.